Title

Transition and Stability of Copolymer Adsorption Morphologies on the Surface of Carbon Nanotubes and Implications on Their Dispersion

Journal

Langmuir, 30(33)

ISSN

0743-7463

Authors

Korayem, Asghar Habibnejad
Barati, Mohammad Reza
Simon, George P
et al.

Publication Date

2014-08-26

DOI

10.1021/la502245s

Peer reviewed

Langmuir

Article

pubs.acs.org/Langmuir

Transition and Stability of Copolymer Adsorption Morphologies on the Surface of Carbon Nanotubes and Implications on Their Dispersion

Asghar Habibnejad Korayem,[†] Mohammad Reza Barati,[‡] George P. Simon,[‡] Tim Williams,[§] Xiao Ling Zhao,[†] Pieter Stroeve,[∥] and Wen Hui Duan*[,†]

[†]Department of Civil Engineering, [‡]Department of Materials Engineering, and [§]Monash Centre for Electron Microscopy, Monash University, Melbourne, Victoria 3800, Australia

[∥]Department of Chemical Engineering and Materials Science, University of California Davis, Davis, California 95616, United States

Supporting Information

ABSTRACT: In this study, the adsorption morphologies as well as stability and transitions of a commercial dispersant copolymer (BYK 9076) on the surface of multiwalled carbon nanotubes (MWCNTs) were studied using Fourier transform infrared and UV−vis spectroscopy, dynamic light scattering, and electron microscopy techniques. The results show that the dispersion of carbon nanotubes in ethanol does not increase continuously with increasing copolymer/CNT ratio, which is correlated with the adsorption morphologies of the copolymer on the CNT surface. At a ratio of copolymer/CNT below 0.5, the morphology is random, shifting to a hemimicelle structure at a ratio from 0.5 to 1.0 while at ratios above 1.0, a cylindrical pattern is seen. The hemimicelle morphology is able to prevent the agglomeration of CNTs when the CNT concentration increases to 8.7 mg/mL, while cylindrical morphology is more efficient and stable to provide dispersion of CNTs at higher concentrations of CNTs.

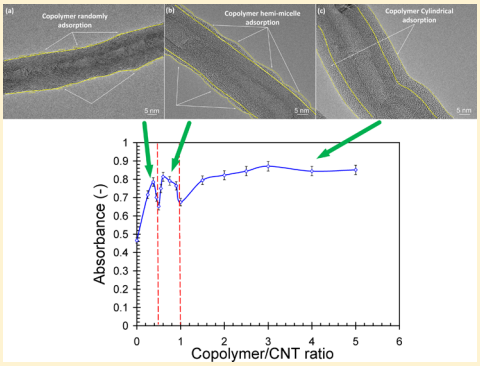

1. INTRODUCTION

Carbon nanotubes (CNTs) have attracted research interest in the field of composites due to their outstanding mechanical properties and high aspect ratio. However, a major barrier for CNT utilization is poor dispersibility and solubility in both aqueous and organic solvents,[1] which limit their applications as nanofillers in the physical property improvement of polymer or cement composites.[2,3] Their high surface area means that high energy surfaces can be reduced by clustering.

Different approaches have been reported in an attempt to achieve an improved uniform dispersion of CNTs, namely (a) mechanical methods such as ultrasonication,[4] high shear mixing,[5] and calendaring,[6] (b) covalent functionalization,[7] and (c) physical surface treatment of CNTs by using dispersants such as surfactants[8−10] and copolymers.[1,11−13] The physical surface treatment of CNTs is of particular interest, as it allows the CNTs to retain excellent mechanical, geometrical, and functional properties such as electrical and thermal conductivity.

Copolymers used as dispersing agents for CNTs usually consist of a hydrophobic block which forms a strong interaction with the CNT surface and a hydrophilic block which provides solubility to the CNTs, by forming steric and electrostatic repulsion forces between the absorbed copolymer on the surface of CNTs,[14] thereby assisting dispersion efficiency.

A comparison of the resultant interfacial morphologies of copolymers with different numbers of blocks, i.e., homopolymer, diblock, and triblock, on the surface of multiwalled CNTs (MWCNTs) in the presence of different solvents is summarized in Table 1. Three different adsorption morphologies of copolymers on the surface of CNTs, i.e., random, hemimicelle, and cylindrical, have been reported and are illustrated in Figure 1. In a random morphology,[15] for example P3HT-*b*-PS, the copolymer molecules self-assemble on the nanotube surface and form a very thin layer (about 2 nm), without any clear structural pattern observed. In the case of PS-*b*-sPI copolymer as a CNT dispersant in water, the CNTs interact with the micellar core directly and a hemimicelle of copolymer molecules is observed. In cylindrical morphology, CNTs are encapsulated with copolymer molecules in a cylindrical pattern where hydrophobic blocks attach to the CNT surface and hydrophobic blocks extend into the solution and provide steric repulsion.[14] For the cylindrical pattern, the copolymer molecules form a thick, dense layer on the CNT surface whereas in random adsorption the surface of CNTs is not fully covered by copolymer.

Received: June 9, 2014
Revised: July 28, 2014
Published: July 31, 2014

Table 1. Comparison of the Interfacial Morphologies of Copolymers with Different Numbers of Blocks on the Surface of CNTs

ref	polymer abbreviation	polymer composition	type of polymer	solvent	CNT concentration (mg/mL)	adsorption morphology
16	P3HT	poly(3-hexylthiophene)	homopolymer	tetrahydrofuran	2.5	cylindrical
17	PS-PB-PMMA	poly(styrene-butadiene-methyl methacrylate)	triblock copolymer	acetone	0.8	cylindrical
15	P3HT-*b*-PS	poly(3-hexylthiophene)-*b*-polystyrene	diblock copolymer	chloroform	2.5-3	random
18	PS-*b*-sPI	polystyrene-*b*-sodium (sulfamate/carboxylate polyisoprene	diblock copolymer	water	0.5	hemimicelle
19	PS-P2VP-*b*-PAA	(polystyrene)22(poly(2-vinylpyridine)-*b*-poly(acrylic acid))22	triblock copolymer	water	2.6	hemimicelle

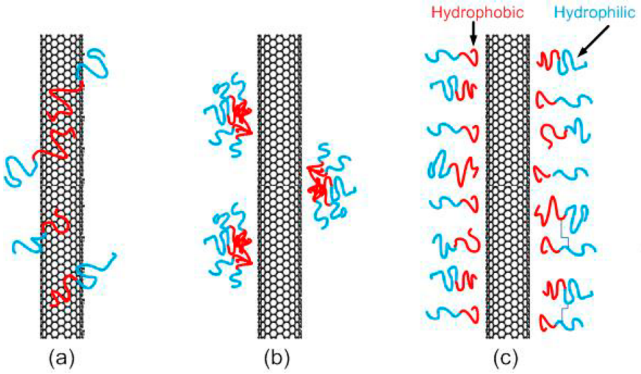

Figure 1. Schematic view of adsorption morphologies of copolymer molecules on the surface of CNTs in aqueous solvents: (a) random, (b) hemimicelle, and (c) cylindrical.

In addition to the copolymers listed in Table 1, BYK 9076, an alkylammonium salt of a high molecular weight copolymer, has been widely adopted to disperse CNTs, especially for the fabrication of CNT-reinforced polymer composites such as polyesters and epoxy nanocomposites.[20] The presence of amine groups as well as carboxylic functionalities[21] makes BYK 9076 a strong dispersant.

On the basis of the discussion in Table 1, the adsorption morphologies have a strong effect on the dispersion of CNTs in aqueous and organic solutions. However, it appears that there have been no investigations reported to date on BYK 9076 for the transition among these morphologies due to the copolymer/CNT ratio and the influence of these morphologies on colloidal stability of CNT dispersion due to the variation of dispersant concentration. It is also of interest to investigate the extent to which the CNT concentration has an effect on the adsorption morphologies in order to assay the stability of these morphologies with regards to CNT concentration.

In the present study, the adsorption morphologies of BYK 9076 on the CNT surface in ethanol as well as their transition and stability are systematically investigated via UV−vis spectroscopy, transmission electron microscopy (TEM), scanning electron microscopy (SEM), and dynamic light scattering (DLS). This work provides a framework to understand the interaction between copolymer and CNTs in ethanol and the implication on the dispersion mechanisms of copolymers. Such an understanding will be helpful for the design, fabrication, and characterization of CNT-reinforced nanocomposites where a good degree of dispersion is required to fully take advantage of the nanosize scale of the primary CNT powders.

2. EXPERIMENTAL SECTION

2.1. Materials. Pristine multiwalled CNTs with 40−60 nm diameter and 5−15 μm length were obtained from NTP, China, with a relative purity of >95 wt %. The dispersing agent was BYK 9076, an alkylammonium salt of a high molecular weight copolymer, supplied by Nuplex Resins, Australia. The solvent was absolute ethanol with 99% purity from Grale Scientific, Australia.

2.2. Sample Preparation and Characterization. Sonication in ethanol was conducted by using a horn sonicator (VCX 500 W) with a cylindrical tip (19 mm end-cap diameter). To prevent a rise in temperature, the solution was placed in a water−ice bath during the sonication process.

To investigate the effect of sonication energy, copolymer/CNT ratios, and CNT concentrations on the interaction among CNTs, copolymer molecules, and ethanol solution, 65 CNT−copolymer−ethanol suspensions were prepared, as shown in Table 2. Exposure to ultrasonic energy was adjusted through different sonication time durations of 5, 10, 15, 30, 45, and 60 min at output power of 25 W.

Table 2. Summary of Various Experimental Conditions Used for Dispersion of CNT−BYK 9076−Ethanol Suspensions

sonication energy (kJ)	copolymer/CNT ratio (mg/mg)	CNT concentration (mg/mL)
	Effect of Sonication Energy	
10, 20, 30, 40, 50, 60, 70, 80, 90, 100, and 110	0.38	1.3
10, 20, 30, 40, 50, 60, 70, 80, 90, 100, and 110	0.5	1.3
10, 20, 30, 40, 50, 60, 70, 80, 90, 100, and 110	1.0	1.3
	Effect of Copolymer/CNT Ratio	
110	0, 0.25, 0.375, 0.45, 0.5, 0.55, 0.6, 0.75, 0.9, 1.0, 1.5, 2.0, 2.5, 3.0, 4.0, 5.0	1.3
	Effect of CNT Concentration	
110	0.6	3.95, 5.93, 7.9, 8.72, 9.49, 9.87, 11.91
110	2.0	3.95, 5.93, 7.9, 8.72, 9.87, 11.91, 15.79, 23.81, 39.47

dx.doi.org/10.1021/la502245s | *Langmuir* 2014, 30, 10035−10042

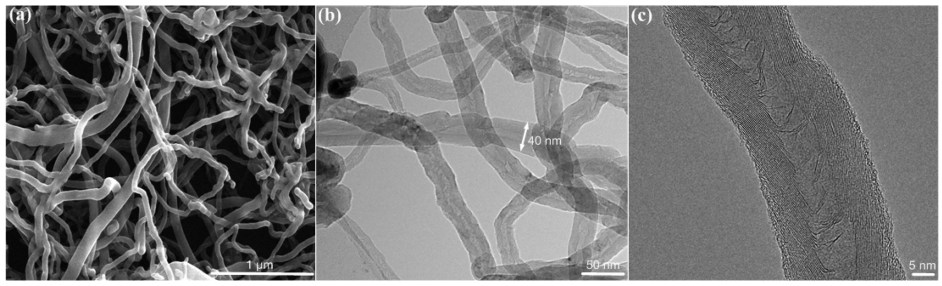

Figure 2. Images of the as-received CNT powders: (a) SEM image and TEM images with (b) low and (c) high magnifications.

The dispersion quality was monitored and quantified using UV−vis spectroscopy. The working principle of UV−vis spectroscopy is that bundled CNTs are not active in the wavelength region between 200 to 900 nm, but individual CNTs are active and show characteristic bands in the UV region. Therefore, the measured absorbance at specific wavelengths can be related to their degree of exfoliation.[22] This method has been widely used for monitoring the exfoliation dynamics of CNTs in solvent media.[22−24] UV−vis measurements were carried out on a Hach DR 5000 spectrophotometer within the wavelength range of 190 to 1100 nm (±1 nm). UV−vis spectra were recorded from the diluted suspensions by a factor of 35 in desired time periods after the sonication treatment. To avoid as much as possible the reagglomeration of dispersed CNTs after sonication treatment, the CNT suspensions were immediately pipetted into a cuvette for UV−vis spectroscopy. The absorbance intensities were measured after baseline subtraction, where the ethanol−copolymer solution spectrum was used to obtain the baseline under the same conditions as for corresponding measurements. For each specimen, three samples were examined and the average of the results was presented.

To morphologically characterize the as-received CNT powders, SEM images were taken using a JEOL 7001F FEG high-resolution scanning electron microscope at 5 kV acceleration voltage. To prepare the SEM sample, the as-received CNT powders were ultrasonically dispersed for 10 min, and then a small amount of CNT suspension was dropped onto a clean silicon substrate mounted on conducting carbon tape. After the ethanol had evaporated, the samples were sputter-coated with a 1 nm layer of gold−palladium.

To observe adsorption morphologies of the copolymer on the surface of CNTs, transmission electron microscopy was utilized. To prepare TEM samples, the CNT suspensions were diluted in absolute ethanol and ultrasonicated for 10 min, and then a droplet of the CNT suspension was pipetted onto a 400 mesh holey-carbon-coated copper grid. After the ethanol had evaporated, the samples were examined using a JEOL 2100F FEG TEM electron microscope operated at an accelerating voltage of 200 kV.

Fourier transform infrared spectroscopy (FTIR) was used for chemical identification of different types of functional groups that exist in BYK 9076. Several drops of highly viscous BYK 9076 solution were dropped onto a KBr aperture plate and sandwiched under another aperture plate to prepare the FTIR sample. FTIR analysis of the samples was conducted using a Thermo Scientific instrument. The analysis was performed at wave numbers from 400 to 4000 cm^{-1}.

The zeta potential is an important indicator of ionically stabilized colloid systems. Greater magnitude (usually ±25 mV) of the zeta potential endows the colloid system with an improved stability against coagulation. To determine the zeta potential and the hydrodynamic size of CNTs in suspensions, a ZetaSizer Nano ZS (Malvern Instrument Ltd., UK) instrument, which uses dynamic light scattering, was applied. All CNT suspensions were equilibrated at a temperature of 25 °C for 2 min before measurements. To check the reproducibility of the hydrodynamic size and zeta potential values, three sets of measurements were taken for each sample, and the mean of the three experiments and resultant standard deviation were then reported.

3. RESULTS AND DISCUSSION

3.1. Morphology of As-Received CNT Powder and Functional Groups of BYK 9076. Figure 2 shows SEM and TEM images of the as-received CNTs, produced by the chemical vapor deposition (CVD) method,[3] which have diameters ranging from 40 to 60 nm and a much entangled morphology. The length of CNTs varies from about 5 to 15 μm, as indicated by the supplier. TEM images with high magnification revealed that the as-received CNTs have a cup-stacked structure.[25] The number of CNT walls, which are clearly visible in Figure 2c, is about 18. Due to the strong van der Waals (vdW) interactions of CNTs, there is a highly dense network of CNTs in the as-received CNT powders.

The FTIR spectrum of BYK 9076 is shown in Figure 3. The peaks at ∼2924 and ∼2854 cm^{-1} are attributed to the

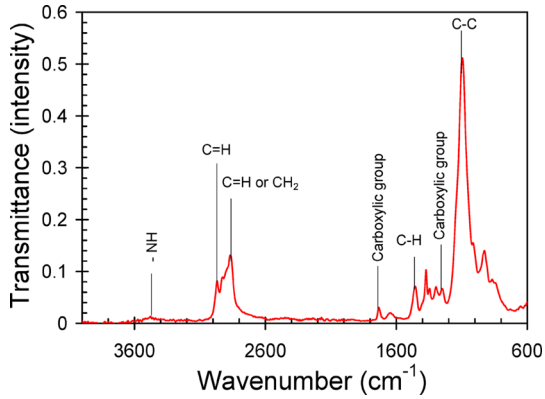

Figure 3. FTIR spectrum of BYK 9076 copolymer.

asymmetric and symmetric stretching vibrations of the (CH_2) group. The peak located at ∼1711 cm^{-1} corresponds to the stretching vibration of the (C═O) group. Furthermore, the peaks at 1250 cm^{-1} and 1729 cm^{-1} can be related to the presence of carboxylic groups on the structure of BYK 9076. Moreover, the characteristic peak at 3500 cm^{-1} can be assigned to the amine group. The presence of the amine group in addition to the carboxylic groups in the molecule structure can induce a bifunctional characteristic in BYK 9076, which can provide two sites for dispersion of CNTs.

3.2. Effect of Ultrasonication Energy. Figure 4a shows the UV−vis spectrum for the CNT−copolymer solutions after 1 and 15 min ultrasonication at 1.5 kJ and 21.2 kJ, respectively. After sonication, the absorbance spectrum of the CNT solutions shows a peak at around 260 nm corresponding to individual CNTs. A similar peak at 260 nm is reported for 1 wt % CNTs dispersed in ethanol using BYK 2150 copolymer.[12] A longer sonication time (15 min) results in a higher absorbance.

dx.doi.org/10.1021/la502245s | Langmuir 2014, 30, 10035−10042

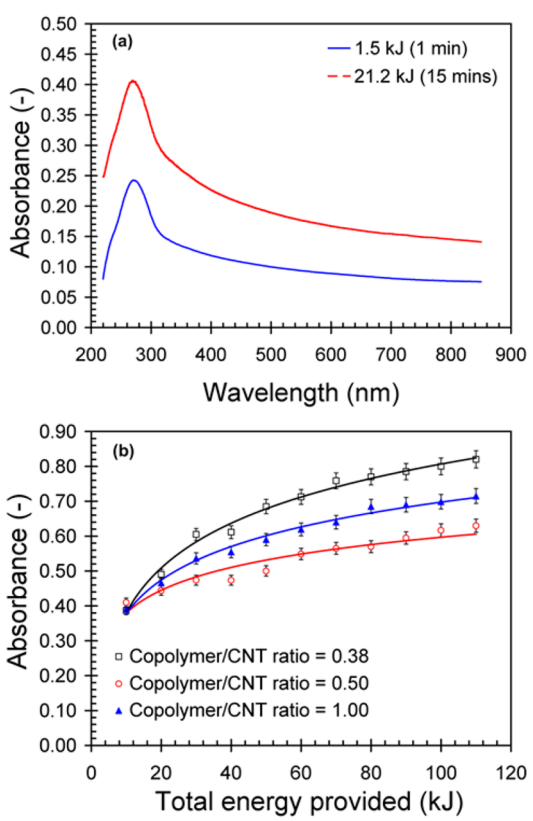

Figure 4. (a) Typical UV−vis spectrum of 0.16 wt % CNT−0.08 wt % surfactant solution for different sonication times and (b) the effect of copolymer/CNT ratio on the peak absorbance of 0.16 wt % CNT in ethanol as a function of sonication energy.

This shows that ultrasonication can indeed overcome the vdW interactions in the CNT bundles and leads to their disentanglement and dispersion. Similar trends are reported for ultrasonic dispersion of CNTs in water with the aid of sodium dodecyl sulfate (SDS).[24] The results indicate that during sonication, CNTs are gradually exfoliated and disentangled from aggregates and bundles and stabilized by SDS.

Figure 4b shows the maximum absorbance at 260 nm as a function of the sonication energy up to 110 kJ for 60 min sonication time, allowing monitoring of the dispersion degree of 0.16 wt % CNT in ethanol with different ratios of copolymer BYK 9076 over CNTs, i.e., 0.38, 0.5, and 1.0. The general trends in the variation of UV absorbance versus sonication energy for all CNT−copolymer solutions appear to be similar. After the initiation of the sonication process, absorbance and sonication energy show a curvilinear relationship. When the level of sonication energy is relatively high, the absorbance reaches a plateau, which corresponds to the maximum achievable degree of dispersion of the CNTs in the ethanol−copolymer solutions.

Interestingly, higher copolymer/CNTs ratios do not lead to greater absorbance or improved dispersion. The absorbance for a ratio of 1.0 is consistently higher than that of 0.5 but lower than that of 0.38. The results show that absorbance (or the CNT dispersion) is not only a function of the sonication energy but also other factors such as the ratio between CNT and copolymer which may influence the degree of CNT dispersion.[26]

3.3. Effect of Copolymer−CNT Ratio. Figure 5 shows the maximum absorbance (the peak at 260 nm) as a function of

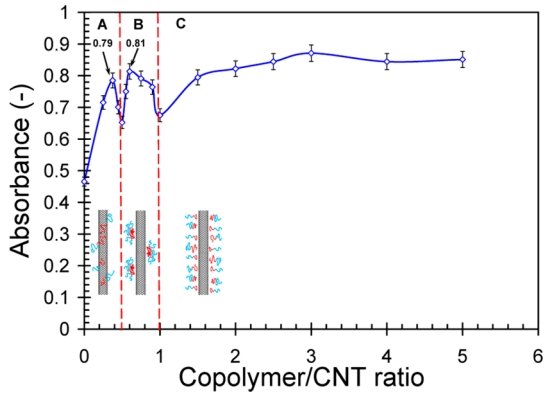

Figure 5. Effect of the copolymer/CNT ratio on the CNT dispersion and its effect on the nature of the copolymer adsorption process: stage A, random adsorption; stage B, hemimicelle adsorption; stage C, cylindrical adsorption.

copolymer/CNT ratio, with the sonication energy held constant at 110 kJ. The absorbance does not monotonically increase with increasing copolymer/CNT ratio. Instead, there are two local peaks, i.e., 0.79 and 0.81, at ratios of 0.38 and 0.6, respectively, followed by a plateau along the absorbance curve. The evolution of the absorbance can be divided into three stages based on these peaks, i.e., stages A, B, and C.

Stage A is within the ratios of copolymer/CNT between 0 and 0.5. At this stage, the absorbance linearly increases with the increasing copolymer/CNT ratio from 0 to 0.38. After reaching the peak, the absorbance linearly decreases with copolymer/CNT ratio from 0.38 to 0.5. This variation of absorbance can be linked to the morphology of the copolymers adsorbed on the surface of CNTs. As shown in the TEM image on the sample with the copolymer/CNT ratio of 0.25 in Figure 6a, random adsorption onto the CNT surface is proposed for the morphology of copolymers. At this stage, the number of copolymer molecules on the CNT surface is relatively small. Prior to the peak of copolymer/CNT ratio at 0.38, there is sufficient space on the CNT surface to accommodate these adsorbed copolymers. The morphology is randomly oriented, and no specific structural pattern can be observed. Therefore, increasing the copolymer/CNT ratio from 0 to 0.38 will have a positive effect on the CNT dispersions, as indicated by the improved absorbance from 0.47 to 0.79. After the peak at 0.38, further increases in the copolymer/CNT ratio causes the adsorption morphology to transit from a random pattern to a hemimicelle morphology. As reported for SDS molecules[26] on CNTs, the interaction energy between CNT and surfactant molecules will be reduced during this transition, and therefore the absorbance also decreases from 0.79 to 0.65, even though the copolymer/CNT ratio increases.

Stage B is in the range of 0.5 to 1.0 copolymer/CNT ratio. A peak of absorbance is observed at a ratio of 0.6. The absorbance increases prior to the peak and decreases thereafter, which can be explained by a change in the adsorption morphology. As shown in the TEM image of the sample with 0.6 copolymer/CNT ratio Figure 6b, the hemimicelle pattern of the adsorption morphology can be clearly observed. The hemimicelle pattern of coated BYK onto the CNT surface leads to the formation of bead-string-shaped CNTs. At this stage, more copolymer

dx.doi.org/10.1021/la502245s | Langmuir 2014, 30, 10035−10042

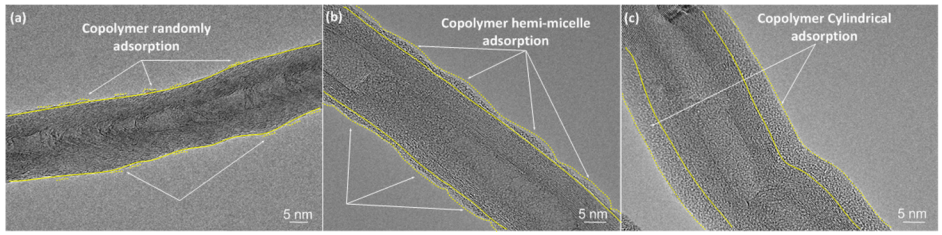

Figure 6. Morphology of the copolymer surrounding the surface of a CNT: (a) random adsorption with 0.25 copolymer/CNT ratio, (b) hemimicelle adsorption with 0.6 copolymer/CNT ratio, and (c) cylindrical adsorption with 5.0 copolymer/CNT ratio.

molecules are available to adsorb on the surface of CNTs, when compared with stage A. More hydrophobic chains of copolymer molecules attach to the CNT surface, the hydrophilic chains thus have less chance to orient on the CNT surface and extend into the solvent, and a hemimicelle pattern is formed.

Increasing the concentration of the copolymer/CNT ratio from 0.5 to 0.6 in stage B not only enables more hydrophobic chains of copolymer molecules to attach to the CNT surface, it also causes a gradual increase of free copolymer molecules in the solution. Increased free copolymer in the solution finally leads to micelle formation when the concentration reaches the critical micellar concentration (cmc). The hydrodynamic size and zeta potential of the pure BYK copolymer−ethanol solution in the absence of CNTs to roughly estimate the cmc of BYK 9076 are presented in the Supporting Information, Table S1 and Figure S1. Increasing the free copolymer molecules in ethanol leads to micelle formation when the concentration reaches 0.78 mg/mL used for CNT/copolymer ratio of 0.6. The concentrations beyond the cmc induce an uncompensated force that results in a depletion attraction between adjacent CNTs, leading to the flocculation of dispersed CNTs. Hence, a reduction in the absorbance value with increasing the copolymer/CNT ratio from 0.6 to 1 can be observed.

Similar trends for stage B in this study have been observed for starlike amphiphilic block copolymers with PPO−PEO segments (AP432) where the absorbance intensity passed through a maximum at an AP432 concentration of 0.5 wt % (exceeding the cmc of AP432) and then decreased.[1] In addition, similar phenomena have also been observed for CNT-F127 (PEO-PPO-PEO triblock copolymers) composites by Monteiro-Riviere et al.[27] Their results indicated that F127, added at low percentages, had a positive effect on the CNT debundling, but when the concentration of F127 reached 5 wt %, larger agglomerates were present, resulting in a reduction of absorbance in the UV−vis spectrum.[27]

When the copolymer/CNT ratio increases to more than 1.0, the curve goes into stage C. The absorbance increases with increasing copolymer/CNT ratio from 1.0 to 3.0 and is followed by a plateau. As shown in the TEM image of the sample with 5.0 copolymer/CNT ratio (Figure 6c), the adsorption morphology of copolymer molecules is a cylindrical pattern, with the thickness of the cylindrical wall of copolymer being around 5 nm. At this stage, a larger number of hydrophobic chains adhere to the CNT surface via physical interactions, and most of hydrophilic chains extend into the solvent.

The experimentally observed different absorbance morphologies with increasing copolymer/CNT ratios can also be explained on the basis of electrostatic interactions between the hydrophobic part and the hydrophilic part in the chemical structure of BYK 9076 on the CNT surface. By adding limited amounts of BYK 9076 (copolymer/CNT ratio <0.5), large available area exists to adsorb the copolymer on the CNT surface, and BYK 9076 molecules randomly orient themselves in such a fashion that hydrophobic tail groups face toward the nanotube surface while hydrophilic head groups face toward the aqueous phase, producing a lowering of the nanotube/ethanol interfacial tension. Therefore, the random adsorption morphology can be observed for a copolymer/CNT ratio of less than 0.5. With an increase in the copolymer concentration (0.5 < ratio <1), more free copolymer molecules were absorbed onto the CNT surface through their hydrophobic tails. Because of the long alkyl chain and bulky headgroup of the adjoining copolymer molecules, BYK copolymer was able to lie flat on the CNT surface along the length of the CNT. Similar phenomena have also been suggested based on molecular dynamics simulation for CNT−poly(3-hexylthiophene) composites by Boon et al.[16] They demonstrated that the first chain adsorbs flat on the CNT surface. Due to the small curvature radius of the CNT, copolymer molecules are probably unable to fully wrap around the CNT. Hence, some part of the CNT surface remains uncoated by copolymer. As a result, bead-string-shaped CNTs form at 0.6 copolymer/CNT ratio as shown in the TEM image of hemimicelle morphology in Figure 6b. As shown in Table 3, when the copolymer/CNT ratio increases from 0.6 to 1, the hydrodynamic sizes increase from 849 ± 2 nm to 932 ± 38 nm. This result agreed well with the reduction in the absorbance in the UV−vis spectrum (Figure 5) where the flocculation of dispersed CNTs occurred. Beside this, the available area to absorb the BYK on the CNT surface decreases with a further increase in the BYK concentration. Thus, some anionic hydrophobic parts remain unattached in the vicinity of the CNT surface. As a result, the positive zeta potential for copolymer/CNT ratio of 0.6 decreases to near zero and becomes negatively charged. The electrostatic interaction between the positively charged hydrophilic head and hydrophobic part bends the BYK hydrocarbon chains. This is energetically favorable for increasing the binding energy and surface coverage of the BYK copolymer onto the CNT surface.

Table 3. Zeta Potential and Hydrodynamic Size Values at Different Copolymer/CNT Ratios

copolymer/CNT ratio	zeta potential value (mV)	hydrodynamic size (nm)
0.6	14.0 (±1.4)[a]	849 (±2)
1	−1.5 (±5.1)	932 (±38)
3.7	7.0 (±3.1)	689 (±12)

[a]Numbers in parentheses represent the standard deviation values.

With a further increase in BYK concentration (ratio >1), the available area to deliver and attach the BYK on the CNT

dx.doi.org/10.1021/la502245s | *Langmuir* 2014, 30, 10035−10042

surface is reduced and the number of unattached anionic hydrophobic parts increases proportionally. Hence, more repulsive forces will be induced between the anionic hydrophobic parts of two adjacent BYK chains. This repulsive force will prohibit the BYK chain bending and results in the straightordination of BYK chains. As a result, these electrostatic surface interactions between unattached anionic hydrophobic parts on two adjacent BYKs produce the cylindrical morphology and provide the high steric repulsive force to prevent CNT bundling. Thus, the hydrodynamic size of the CNT bundle is reduced from 932 ± 38 nm to 689 ± 12 nm with an increase in the copolymer/CNT ratio from 1 to 3.7, the bead-shaped morphology in Figure 6b disappeared, and BYK copolymer distributed flatly along the CNT surface with a thickness of several nanometers which is clearly indicated in Figure 6c. While the wall of neat CNT in Figure 2c shows a homogeneous dark-gray color, the CNTs coated with a CNT/copolymer ratio of 5.0 have a flat coated layer of BYK copolymer on the surface. In addition to this adsorption mechanism, it is also believed that an increase in the copolymer/CNT ratio beyond the cmc would cause a gradual increase in the size of micelles on the CNT surface. The micelle size grew large enough to incorporate neighboring micelles. Sufficiently large micelles can imbed in the entire structure of the CNT and then form cylindrical morphology on the CNT surface. Thus, not only can the copolymer−CNT interaction predominantly affect the observed different absorbance morphologies with increasing copolymer/CNT ratio, but the formation tendency of the micelles could also contribute to a change in the amount of copolymer adsorption on the CNTs. The sizes of micelles in the pure BYK copolymer−ethanol solution at a concentration of 1.3 mg/mL used for a ratio of 1 are presented in the Supporting Information Figure S2. Although the average sizes of micelles are about 1 μm, there are some large micelles with sizes of about 4 μm. It is indicated that beyond the cmc, the micelles start to grow and form larger micelles, and the CNTs become imbedded within them.

3.4. Effect of CNT Concentration in Ethanol. The CNT concentration with a fixed copolymer/CNT ratio represents the separation distance between individual CNTs within the solvent, which will decrease when the concentration of the CNT increases. It is important to investigate whether the adsorption morphologies discussed in section 3.3 are stable for different CNT concentrations.

The dispersibility and colloidal stability of CNTs in their suspensions is strongly dependent on the hydrodynamic size of the individual CNTs. The average of the hydrodynamic size of the suspensions as a function of CNT concentration is plotted in Figure 7a. When the CNT concentration is relatively small, say smaller than 7.9 mg/mL, the hydrodynamic sizes for the samples with 0.6 and 2.0 copolymer/CNT ratios are about 400 and 600 nm, respectively. The increased hydrodynamic size for higher copolymer/CNT ratios provides additional evidence for the presence of a thicker copolymer coat on the surface of the CNTs. These results are in good agreement with the TEM images results shown in Figure 6, where high copolymer/CNT ratios form a thicker shell on the CNT surfaces.

When the CNT concentration increases up to 7.9 mg/mL, the hydrodynamic size of the sample with 0.6 copolymer/CNT ratio is almost constant. This means that the hemimicelle-oriented copolymer molecules are able to prevent the CNTs from bundling by keeping the CNT separation distance extensive. However, at CNT concentrations between 8.7 to

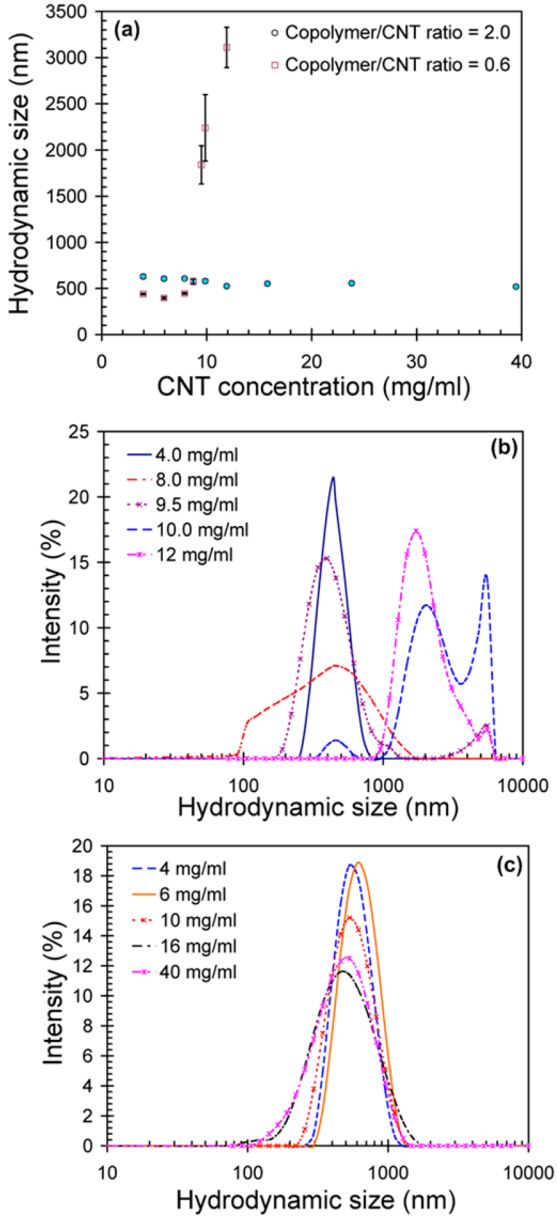

Figure 7. (a) Mean hydrodynamic sizes of CNTs in the suspension, and hydrodynamic size distribution of CNTs at copolymer/CNT ratios of (b) 0.6 and (c) 2.0 as a function of CNT concentration.

11.9 mg/mL, the hydrodynamic size of CNTs increases due to the agglomeration of CNTs. Thus, at high CNT concentration or small CNT separation distance, the hemimicelle morphology is not able to provide sufficient repulsive force against vdW interaction to prevent CNT bundling.

Interestingly, the hydrodynamic size of CNTs in the sample with 2.0 copolymer/CNT ratio is almost constant at about 600 nm. In fact, the CNT suspension with the copolymer/CNT ratio of 2.0 retains their initial hydrodynamic sizes over a broad CNT concentration range. This means that the cylindrical morphology is able to provide a high steric repulsive force to prevent CNT bundling.

Figure 7b and Figure 7c show the hydrodynamic size distribution of CNT suspension with different copolymer/CNT ratios as a function of CNT concentration. To represent a measure of variability in the CNT size distribution in their

dx.doi.org/10.1021/la502245s | Langmuir 2014, 30, 10035−10042

suspensions, the polydispersity index (PdI) is measured. The PdI of CNT suspensions is tabulated in Table 4.

Table 4. Polydispersity Index and Zeta Potential of CNTs in the Suspensions as a Function of CNT Concentration at the Copolymer/CNT Ratios of 0.6 and 2.0

copolymer/CNT ratios	CNT concentration (mg/mL)	polydispersity index	zeta potential (mV)
0.6	4	0.11 (±0.06)[a]	14.4 (±0.5)
	6	0.21 (±0.04)	–
	8	0.30 (±0.05)	–
	8.7	0.30 (±0.04)	16.6 (±1.5)
	9.5	0.30 (±0.06)	–
	10	0.35 (±0.05)	–
	12	0.31 (±0.10)	14.2 (±0.5)
2.0	4	0.28 (±0.04)	–
	6	0.19 (±0.12)	–
	8	0.25 (±0.06)	–
	8.7	0.25 (±0.03)	29.1 (±0.7)
	10	0.25 (±0.04)	30.7 (±4.0)
	12	0.28 (±0.07)	28.1 (±1.2)
	16	0.26 (±0.01)	37.0 (±1.0)
	24	0.27 (±0.04)	33.3 (±0.8)
	40	0.24 (±0.02)	36.4 (±1.7)

[a]Numbers in parentheses represent the standard deviation values.

For the samples with 0.6 copolymer/CNT ratio, the PdI increases by about a factor 3 from 0.11 (±0.06) to 0.31 (±0.10) as the CNT concentration increases. The results demonstrate that a peak broadening as well as peak splitting occurs with increasing CNT concentration from 4 mg/mL to 12 mg/mL as shown in Figure 7b.

The broadening and splitting of the size distribution curves for higher CNT concentrations indicates the progressive agglomeration of CNTs which arises from the existence of hemimicelle morphology in a ratio of 0.6. However, all CNT suspensions with different CNT concentrations at a copolymer/CNT ratio of 2.0 show a single size distribution peak as shown in Figure 7c, and they have almost identical values of PdI in Table 4. As shown in Table 4, the PdI value of 0.28 (±0.04) for a CNT concentration of 4 mg/mL remains relatively constant, with no significant changes, to a value of 0.24 (±0.02) for a high CNT concentration of 40 mg/mL. The PdI values are smaller in comparison to the copolymer/CNT ratio of 0.6 which renders narrower CNT size distribution. Such stability in the hydrodynamic size and low PdI values in these CNT suspensions can be ascribed to the cylindrical adsorption morphology of the copolymer on the CNT surface at the copolymer/CNT ratio of 2.0.

BYK 9076 adsorbs on the CNT surface in the way that alkyl groups (hydrophobic portion) in the molecular structure of BYK 9076 attach to the CNT surface, and the amine and carboxylic groups (hydrophilic portions) point to the ethanol. Thus, after BYK 9076 adsorption, the surface charge of the CNTs becomes positive, which can arise from the alkyl cations. The CNTs with a copolymer/CNT ratio of 0.6 have a zeta potential 16.6 ± 1.5 mV and 14.2 ± 0.5 mV for CNT concentrations of 8.7 and 12 mg/mL, respectively. For CNT coated with a copolymer/CNT ratio of 2.0, the zeta potential increases to 29.1 ± 0.7 mV and 28.1 ± 1.2 mV for CNT concentrations of 8.7 and 12 mg/mL, respectively. The increasingly positive zeta potential for copolymer/CNT ratio of 2.0 is able to improve the dispersibility of CNTs in ethanol, which is in agreement with the results from UV−vis spectroscopy. This indicates the important role of BYK 9076 in the dispersion of CNTs as a stabilizer agent through electrostatic repulsion.

The aforementioned results reveal that in addition to a strong steric repulsion from the lengthy hydrocarbon tail in the molecular structure of BYK 9076, the higher surface charge provides an additional repulsive force to increase the dispersion ability of the CNTs. Therefore, although each molecule of the branched AP432 copolymer can interact with much smaller bundles or even individual CNTs,[1,28] BYK 9076 could create a stronger steric and electrostatic repulsion forces for CNT dispersion. The disentanglement of CNTs by AP432 was achieved under sonication energy of 720 kJ,[1] while much lower sonication energy was used for dispersion of CNTs in this study in the presence of BYK 9076 as a dispersant. Moreover, unlike the branched AP432 copolymer and linear copolymers such as Pluronics L64 triblock and F127 copolymers,[1] the bifunctional characteristic in BYK 9076 can enhance the coordination degree with the graphitic surface of CNTs.[21] Because BYK 9076 copolymers have a much lower cmc of 0.78 mg/mL and could form much bigger micelles compared with linear copolymers (192 mg/mL for L64 triblock[28]), they can be a good candidate to achieve a high level of CNT dispersion. These effects result in one point; that is, BYK 9076 copolymers hold great potential in dispersing CNTs at a much lower concentration and can give smaller CNT bundles.

4. CONCLUSIONS

The adsorption morphologies of copolymer molecules on the surface of carbon nanotubes and their transition and stability were investigated using FTIR and UV−vis spectroscopy, microscopy, and hydrodynamic size analysis. The CNT dispersion depends not only on the copolymer concentration but also on the morphology of the copolymers on the surface of the CNTs. Dispersion does not increase continuously with an increase in the copolymer/CNT ratio; it fluctuates with the copolymer/CNT ratio, and the dispersibility of copolymer can be linked to the adsorption morphologies on the CNT surface.

The copolymer adsorption morphology on CNTs is also dependent on the copolymer/CNT ratio. For BYK 9076, an alkylammonium salt of a high molecular weight copolymer and the dispersant used in this study, at a ratio below 0.5, the morphology is random. At a moderate ratio from 0.5 to 1.0, the morphology follows the hemimicelle pattern, and at a high ratio above 1.0 it changes to a cylindrical pattern. Hemimicelle morphologies can prevent the agglomeration of CNTs when the CNT concentration increases to 8.7 mg/mL, while the cylindrical morphology is more efficient, stable, and able to provide improved dispersions of the CNTs at higher concentrations of CNTs.

Good agreement is obtained between the mean hydrodynamic size and zeta potential values of CNT suspensions obtained by the DLS technique and from UV−vis analysis results. The CNTs coated with a copolymer/CNT ratio of 2.0 show narrower size distribution with a smaller polydispersity index in comparison to a ratio of 0.6. Thus, to achieve highly dispersed CNTs in the ethanol−BYK 9076 suspension, the copolymer/CNT ratio in the suspension should be 2.0. It is also demonstrated that the dual roles of BYK 9076 in the dispersion of CNTs in the ethanol are through steric repulsion as well as electrostatic repulsion.

dx.doi.org/10.1021/la502245s | Langmuir 2014, 30, 10035−10042

■ ASSOCIATED CONTENT

Supporting Information

Additional information as noted in the text. This material is available free of charge via the Internet at http://pubs.acs.org.

■ AUTHOR INFORMATION

Corresponding Author

*E-mail: wenhui.duan@monash.edu.

Notes

The authors declare no competing financial interest.

■ ACKNOWLEDGMENTS

The authors are grateful for financial support from the Australian Research Council in conducting this study. A.H.K. thanks the Ministry of Science, Research and Technology of Iran, for financial support. The authors acknowledge the cooperation of Nuplex Resins, Australia, for the supply of BYK dispersants. We acknowledge the use of the facilities within the Monash Centre for Electron Microscopy.

■ REFERENCES

(1) Xin, X.; Xu, G.; Zhao, T.; Zhu, Y.; Shi, X.; Gong, H.; Zhang, Z. Dispersing carbon nanotubes in aqueous solutions by a starlike block copolymer. *J. Phys. Chem. C* **2008**, *112*, 16377−16384.

(2) Chen, S. J.; Collins, F. G.; Macleod, A. J. N.; Pan, Z.; Duan, W. H.; Wang, C. M. Carbon nanotube−cement composites: A retrospect. *IES J. Part A: Civil Struct. Eng.* **2011**, *4*, 254−265.

(3) Coleman, J. N.; Khan, U.; Blau, W. J.; Gun'ko, Y. K. Small but strong: A review of the mechanical properties of carbon nanotube−polymer composites. *Carbon* **2006**, *44*, 1624−1652.

(4) Habibnejad Korayem, A.; Barati, M. R.; Simon, G. P.; Zhao, X. L.; Duan, W. H. Reinforcing brittle and ductile epoxy matrices using carbon nanotubes masterbatch. *Composites, Part A* **2014**, *61*, 126−133.

(5) Sandler, J.; Shaffer, M. S. P.; Prasse, T.; Bauhofer, W.; Schulte, K.; Windle, A. H. Development of a dispersion process for carbon nanotubes in an epoxy matrix and the resulting electrical properties. *Polymer* **1999**, *40*, 5967−5971.

(6) Sumfleth, J.; Prehn, K.; Wichmann, M. H. G.; Wedekind, S.; Schulte, K. A comparative study of the electrical and mechanical properties of epoxy nanocomposites reinforced by CVD- and arc-grown multi-wall carbon nanotubes. *Compos. Sci. Technol.* **2010**, *70*, 173−180.

(7) Ma, P. C.; Mo, S. Y.; Tang, B. Z.; Kim, J. K. Dispersion, interfacial interaction and re-agglomeration of functionalized carbon nanotubes in epoxy composites. *Carbon* **2010**, *48*, 1824−1834.

(8) Wang, H.; Zhou, W.; Ho, D. L.; Winey, K. I.; Fischer, J. E.; Glinka, C. J.; Hobbie, E. K. Dispersing single-walled carbon nanotubes with surfactants: A small angle neutron scattering study. *Nano Lett.* **2004**, *4*, 1789−1793.

(9) Wenseleers, W.; Vlasov, I. I.; Goovaerts, E.; Obraztsova, E. D.; Lobach, A. S.; Bouwen, A. Efficient isolation and solubilization of pristine single-walled nanotubes in bile salt micelles. *Adv. Funct. Mater.* **2004**, *14*, 1105−1112.

(10) Islam, M. F.; Rojas, E.; Bergey, D. M.; Johnson, A. T.; Yodh, A. G. High weight fraction surfactant solubilization of single-wall carbon nanotubes in water. *Nano Lett.* **2003**, *3*, 269−273.

(11) Shin, H.-i.; Min, B. G.; Jeong, W.; Park, C. Amphiphilic block copolymer micelles: New dispersant for single wall carbon nanotubes. *Macromol. Rapid Commun.* **2005**, *26*, 1451−1457.

(12) Zhao, L.; Gao, L. Stability of multi-walled carbon nanotubes dispersion with copolymer in ethanol. *Colloids Surf., A* **2003**, *224*, 127−134.

(13) Mountrichas, G.; Tagmatarchis, N.; Pispas, S. Synthesis and solution behavior of carbon nanotubes decorated with amphiphilic block polyelectrolytes. *J. Phys. Chem. B* **2007**, *111*, 8369−8372.

(14) Lewis, J. A. Colloidal processing of ceramics. *J. Am. Ceram. Soc.* **2000**, *83*, 2341−2359.

(15) Zou, J.; Liu, L.; Chen, H.; Khondaker, S. I.; McCullough, R. D.; Huo, Q.; Zhai, L. Dispersion of pristine carbon nanotubes using conjugated block copolymers. *Adv. Mater.* **2008**, *20*, 2055−2060.

(16) Boon, F.; Desbief, S.; Cutaia, L.; Douhéret, O.; Minoia, A.; Ruelle, B.; Clément, S.; Coulembier, O.; Cornil, J.; Dubois, P.; Lazzaroni, R. Synthesis and Characterization of Nanocomposites Based on Functional Regioregular Poly(3-hexylthiophene) and Multiwall Carbon Nanotubes. *Macromol. Rapid Commun.* **2010**, *31*, 1427−1434.

(17) Périé, T.; Brosse, A.-C.; Tencé-Girault, S.; Leibler, L. Nanostructured films and composites from carbon nanotubes dispersed by ABC block terpolymers in selective solvent. *Polymer.* **2011**, *52*, 3065−3073.

(18) Mountrichas, G.; Tagmatarchis, N.; Pispas, S. Synthesis and solution behavior of carbon nanotubes decorated with amphiphilic block polyelectrolytes. *J. Phys. Chem. B* **2007**, *111*, 8369−8372.

(19) Iatridi, Z.; Tsitsilianis, C. pH responsive MWCNT−star terpolymer nanohybrids. *Soft Matter.* **2013**, *9*, 185−193.

(20) Nouranian, S.; Toghiani, H.; Lacy, T. E.; Pittman, C. U.; Dubien, J. Dynamic mechanical analysis and optimization of vapor-grown carbon nanofiber/vinyl ester nanocomposites using design of experiments. *J. Compos. Mater.* **2011**, *45*, 1647−1657.

(21) Shafieizadegan Esfahani, A. R.; Katbab, A. A.; Dehkhoda, P.; Karami, H. R.; Barikani, M.; Sadeghi, S. H. H.; Ghorbani, A. Preparation and characterization of foamed polyurethane/silicone rubber/graphite nanocomposite as radio frequency wave absorbing material: The role of interfacial compatibilization. *Compos. Sci. Technol.* **2012**, *72*, 382−389.

(22) Grossiord, N.; Loos, J.; Meuldijk, J.; Regev, O.; Miltner, H. E.; Van Mele, B.; Koning, C. E. Conductive carbon-nanotube/polymer composites: Spectroscopic monitoring of the exfoliation process in water. *Compos. Sci. Technol.* **2007**, *67*, 778−782.

(23) Grossiord, N.; Regev, O.; Loos, J.; Meuldijk, J.; Koning, C. E. Time-dependent study of the exfoliation process of carbon nanotubes in aqueous dispersions by using UV−visible spectroscopy. *Anal. Chem.* **2005**, *77*, 5135−5139.

(24) Yu, J.; Grossiord, N.; Koning, C. E.; Loos, J. Controlling the dispersion of multi-wall carbon nanotubes in aqueous surfactant solution. *Carbon* **2007**, *45*, 618−623.

(25) Yokozeki, T.; Iwahori, Y.; Ishiwata, S. Matrix cracking behaviors in carbon fiber/epoxy laminates filled with cup-stacked carbon nanotubes (CSCNTs). *Composites, Part A* **2007**, *38*, 917−924.

(26) Duan, W. H.; Wang, Q.; Collins, F. Dispersion of carbon nanotubes with SDS surfactants: a study from a binding energy perspective. *Chem. Sci.* **2011**, *2*, 1407−1413.

(27) Monteiro-Riviere, N. A.; Inman, A. O.; Wang, Y. Y.; Nemanich, R. J. Surfactant effects on carbon nanotube interactions with human keratinocytes. *Nanomedicine (N. Y., NY, U. S.)* **2005**, *1*, 293−299.

(28) Xin, X.; Xu, G.; Zhang, Z.; Chen, Y.; Wang, F. Aggregation behavior of star-like PEO−PPO−PEO block copolymer in aqueous solution. *Eur. Polym. J.* **2007**, *43*, 3106−3111.